International Journal of Advanced Research in Engineering Technology & Science
ISSN: 2349-2819
Email: editor@ijarets.org Volume-6, Issue-7 July- 2019 www.ijarets.org

EFFECTS OF SURFACE ROUGHNESS ON TWO AND THREE-DIMENSIONAL MFD BOUNDARY LAYERS

Dr. Pankaj Mathur
Associate Professor
Government College, Tonk(Rajasthan)

Dr. P. R. Parihar
Associate Professor
S.P.C. Government College, AJMER(Rajasthan)

ABSTRACT

The purpose of this study work is to investigate how the surface roughness of two-dimensional (2D) and three-dimensional (3D) multi-function displays (MFDs) affects the boundary layer properties of such displays. In MFDs, the surface roughness may have a major impact on the flow behavior, the boundary layer separation, and the heat transfer. This research will evaluate the influence of different surface roughness characteristics, such as roughness height and spatial distribution, on the performance of 2D and 3D MFD boundary layers by a mix of experimental measurements and numerical simulations. Roughness height and spatial distribution are two examples of surface roughness factors that will be investigated. The results will give critical insights that will be necessary for the design and optimization of MFD surfaces, which will ultimately result in enhanced display efficiency and lower energy usage.

Key word: *boundary layer, roughness.*

INTRODUCTION

A key noise source for wind turbines and airplanes is the aerodynamic noise that is created by the convection of a turbulent boundary layer passing a sharp trailing edge of an airfoil. The boundary-layer characteristics at the trailing edge are impacted by the position of transition onset, which has an effect on the intensity of far-field noise as well as its spectral distribution. This has a significant bearing on the far-field noise's spectral distribution. The uncertainty in the transition site has an influence on the comparability of tests that were carried out in various wind tunnels, which may have differences in the intensity of freestream turbulence and in the manner that the process of laminar to turbulent transition is created in the boundary-layer flow. Within the framework of the BANC series of workshops hosted by the AIAA, Herr et al and Herr and Kamruzzaman provided a comprehensive comparison of numerical simulations and wind-tunnel measurements of trailing-edge noise for both symmetric and cambered airfoils. The results showed a difference on the far-field noise level of approximately 3 dB between experimental results even when obtained with the same setup and nominal flow conditions. In controlled wind tunnel investigations, surface roughness components are traditionally utilized as devices to induce a transition from laminar to turbulent flow. Two-dimensional roughness elements (such as wires, steps, and gaps), and three-dimensional isolated or dispersed roughness are the two primary categories that are commonly used to classify roughness elements. elements. Two-dimensional roughness elements have an effect on the transition process by amplifying the Tollmien–Schlichting (TS) waves more so in the separation and recovery regions of the transition. in the background of the roughness parts. A rise in the Reynolds number results in a rise in the amplitude of the TS wave which in turn causes a progressive upstream movement of the transition position toward the location of the roughness element. The boundary layer flow experiences a localized spanwise deflection as a result of the presence of three-dimensional roughness components. In the aftermath of roughness elements, counterrotating streamwise vortex pairs are created. This results in the production of low- and high-speed streaks, which modify the

surface shear in the spanwise direction. Once the streak amplitude above a threshold point, the streak will be vulnerable to a secondary instability in the form of either sinuous or varicose modulation, which will finally lead to breakdown into turbulence. This secondary instability may take the shape of either a sinusoidal or a varicose pattern.Distributed roughness elements, as opposed to isolated roughness elements, are utilized more often as a tripping device in wind-tunnel studies owing to their efficiency in promoting transition and increased spanwise uniformity of the downstream turbulent flow. This is because distributed roughness elements improve spanwise uniformity of the downstream turbulent flow. In actuality, the blades of wind turbines are susceptible to erosion from sand or hail, insect deposits, and ice, all of which may contribute to the creation of similarly rough surfaces near to the leading edge. When conducting studies in the wind tunnel at low Reynolds numbers, it is common practice to make use of bigger boundary-layer trips in order to circumvent the sensitivity of airfoil self-noise to the transition site. Large-sized boundary layer trips may introduce coherent flow structures that persist up until the trailing edge, thus altering the streamwise and spanwise correlations of the turbulent boundary layer and affecting trailing-edge noise. This occurs despite the fact that the large-sized boundary layer trips guarantee a fully turbulent boundary layer at the trailing edge. Therefore, in order to effectively forecast the far-field noise, one has to have a solid understanding of, and control over, the position of the transition.

In recent years, acoustic measurements made using microphone arrays have been utilized to study the influence that surface roughness has on trailing-edge noise. Hutcheson and Brooks examined trailingedge noise from a NACA 63-215 airfoil. Over the first 5% of the chord, the boundary layer was tripped with steel grits and serrated tape at a height of 0.29 mm. It was discovered that the noise caused by the trailing edge is the most prominent source of noise in the low-frequency region. On the other hand, at higher frequencies ($f > 12.5$ kHz), the noise source that is attributable to surface roughness near to the leading edge becomes the dominating contributor. Cheng et al. conducted research to determine how the roughness of rotor surfaces that were caused by surface icing affected the wideband noise of the rotors. They came to the conclusion that the height of the surface roughness has an effect on both the thickness of the boundary layer and the turbulence intensity at the trailing edge. A large increase in the amount of trailing-edge noise is produced at frequencies greater than 4 kHz as a direct result of an increase in the turbulence intensity.Acoustic measurements were carried out by Oerlemans et al on a full-scale model of a three-blade wind turbine in order to identify the primary noise contributors.When compared to clean turbine blade circumstances, it was discovered that the overall sound level increased by about 3.6 dB A when the blade was equipped with significantly larger-sized roughness components than the one that was required to promote transition. This was the case when the overall sound level was measured. When the frequency is less than 2 kHz, there is also an increase in the noise source's overall extent.The study that was done up until fairly recently on the influence of distributed surface roughness on boundary-layer transition did not spend enough attention to identifying the association between the flow topology, the underlying transition mechanism, and the far-field noise. This is something that has only happened quite lately. Using a large-eddy simulation, Winkler et al. investigated how the presence of a step and serration trip along the trailing edge of a NACA 6512-63 airfoil affected the amount of trailing-edge noise.

The position of the transition's beginning is greatly impacted by the geometry of the roughness, which ultimately results in distinct flow patterns at the trailing edge and in the airfoil wake. According to the far-field noise forecast, the noise level associated with the step is about 10 decibels (dB) more than the noise level associated with the entire trip. In their recent work, Ribeiro et al. presented the first set of numerical simulations to investigate the effects of sand-grain surface roughness on trailing-edge noise over a NACA 0012 airfoil. These simulations were carried out using a NACA 0012 airfoil. They discovered that by positioning the surface roughness over the leading edge of the airfoil, the far-field noise level may be reduced by 10 decibels when compared to the level produced by the clean airfoil design. A more in-depth characterisation of the flowfield is the focus of the current study, which has as its overarching goal the expansion of our knowledge of various facets. In order to accomplish this goal, measurements were carried

out in an experimental setup that was similar to the one used by Brooks et al. to study the trailing-edge noise of airfoils. Roughness elements with a random distribution were applied to a NACA 0012 airfoil while the angle of attack was set to zero degrees. A zigzag strip with the same height and streamwise length as the distributed roughness patch was tested in order to make a comparison. This is because zigzag strips are also often employed as three-dimensional boundary-layer tripping devices. Using a three-dimensional laser scanner, the distribution of the roughness elements was analyzed, and as a result, a reference geometry was established for use in further computational research. The surface temperature was measured by means of infrared thermography, which made it possible to locate the point at which the change took place. The time-averaged velocity field that was recorded using hot-wire anemometry was used to describe the flow topology upstream of the roughness elements and around the roughness elements themselves. In the frequency domain, the turbulent behavior was elaborated by the turbulent intermittency and the power spectral density. The noise sources were found and quantified with the use of measurements taken with phased microphone arrays, which highlighted the effect of various roughness geometries on the far-field noise.

OBJECTIVES OF THE STUDY

1. To the study of surface roughness.
2. To the study of far-field noise.

A. Current Flow and Available Testing Facilities

Experiments were carried out in the anechoic vertical open-jet wind tunnel that is located inside the Aerodynamics Laboratories of the Aerospace Engineering Faculty at Delft University of Technology. The test portion of the wind tunnel is 0.4 by 0.7 meters squared, which corresponds to a contraction ratio of 15 to 1.This particular segment has a maximum allowable velocity of 42.5 meters per second. When traveling at this speed, the turbulence intensity is less than 0.1%. A homogeneity of 0.5% may be seen over the test portion in terms of the freestream velocity distribution.In the symmetry plane of the test section, a NACA 0012 airfoil measuring 300 millimeters in chord c and 400 millimeters in span b was fitted between the side plates. The angle of attack on the airfoil was set to be 0 degrees. A right-handed reference system is created by introducing a Cartesian system of coordinate axes that is centered at the leading edge of the airfoil. In this system, the x axis is aligned with the airfoil chord, the z axis is oriented along the span, and the y axis is normal to both of them. This creates a right-handed reference system. Figure 1 presents a conceptual drawing of the model's overall configuration for clarity. Honeywell TruStability pressure sensors, numbering twenty-four in total, are used to perform an alignment check on the airfoil.There are twelve pressure sensors placed evenly along each side of the airfoil in the chordwise range of x-c 0.30; 0.70. In order to prevent flow interference between adjacent pressure sensors, they are aligned at an angle of 22 degrees with regard to the chord. The data is acquired at a frequency of 2000 Hz over a period of sixty seconds. Calculating the pressure coefficient differential cp between the two sides of the airfoil at various freestream velocities in order to compare the results with those predicted by XFOIL allows one to establish the angle of attack for the airfoil. As can be seen in Figure 2, the angle of attack is somewhere between 0.15 and 0.1 degrees.

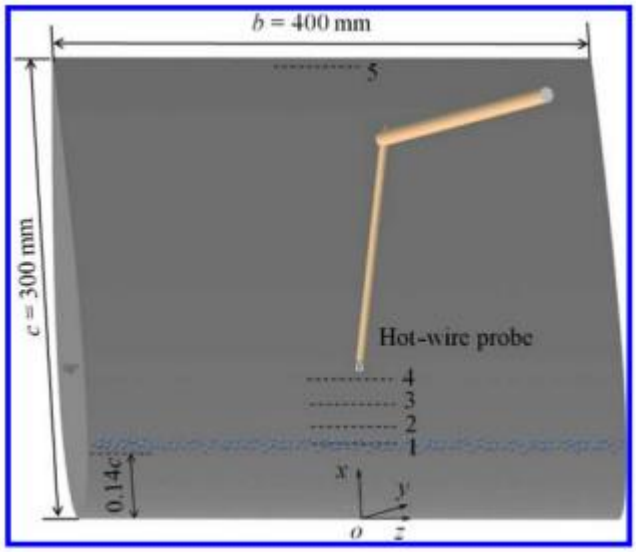

Fig. 1 A diagrammatic representation of the experimental setup. The measurement planes of the hot-wire anemometry are shown by the dashed lines 1–5, which correspond to the coordinates of xc 0.16, 0.19, 0.24, and 0.29, respectively.

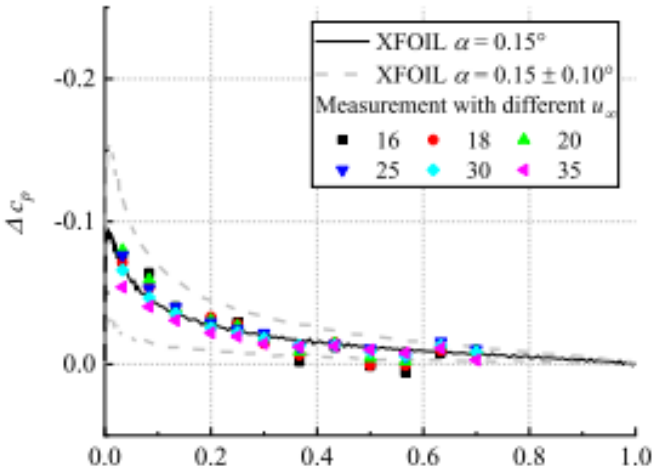

Figure 2 the distribution of the pressure coefficient differential (cp) under a variety of flow circumstances.

Both a zigzag strip and randomly dispersed roughness components were put through their paces as potential boundary-layer tripping mechanisms. On both the suction and pressure sides of the airfoil, the roughness elements were inserted over the chordwise range of 0.14–0.18 on both sides of the airfoil across the whole span.The components that contribute to the dispersed roughness have spherical forms (also known as grit), and their diameters range from 0.3 to 0.1 millimeters on average. Roughness elements are packed in at a density of around two per millimeter on average.A high-speed laser scanner (Micro-Epsilon scanCONTROL 2925, with a maximum frequency of 2 kHz) was used in order to get data on the roughness distribution. It is a tiny device that generates laser sheets and has an optical system built right in so that it can receive the reflected laser light from the surface being targeted. The triangulation of laser lines provides the basis for the scanner's operational methodology. The laser sheet that is created by the scanner crosses across the upper half of the pieces that make up the spherical grit. As a direct consequence of this, the roughness elements are distinguished by their hemispherical form. The laser sheet had its length aligned in the streamwise direction x, and a total of 1280 points were collected in a single streamwise profile. The sheet was 29 millimeters in

length. The focal range of the scanner is enough to accommodate the distance of 651 millimeters (mm) that separates it from the surface of the airfoil. The scan was moved using an in-house traverse control system with a step size of 0.025 mm in the range zc 0.08; 0.08. This allowed for the measurement of the spanwise surface variation.The resolutions of the scanning process along the x, y, and z axes are correspondingly 22, 2, and 25 micrometers. Figure 3 depicts the scanned surfaces on both the top and lower surfaces. As a point of reference, a standard zigzag strip with the same height of 0.3 mm and streamwise extent of 0.04c was used. The angle formed by the zigzag strip at its top is sixty degrees.

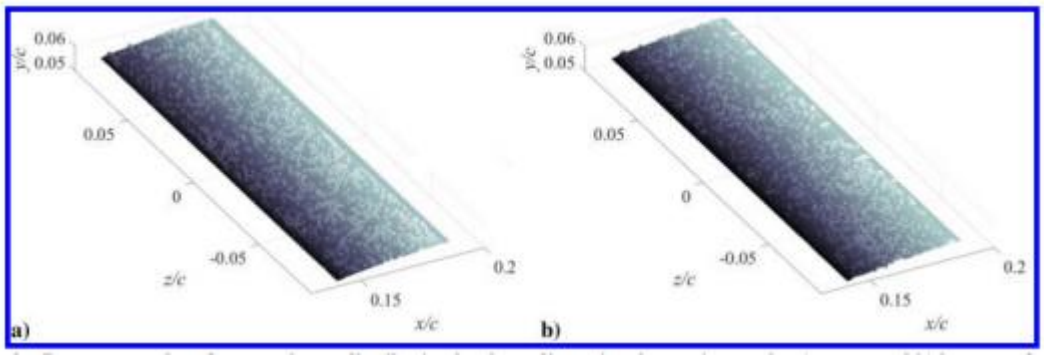

Figure 3 shows the reconstructed surface roughness distribution that was achieved using three-dimensional scanning on the top and lower surfaces, respectively.

CONCLUSION

Extensive research into the effects of surface roughness on two-dimensional (2D) and three-dimensional (3D) MFD (Mean Flow Deflection) boundary layers has shown considerable implications on flow behavior and boundary layer properties. This research was carried out in two dimensions and three dimensions. The result that was reached after doing this comparative research elucidates the impact that surface roughness has on both two-dimensional and three-dimensional boundary layers. In the context of 2D boundary layers, surface roughness is responsible for the introduction of disturbances that interact with the flow. As a result, there is an increase in the amount of drag and energy lost due to the skin friction. The surface's imperfections cause the laminar sublayer to become disrupted and encourage an early transition to turbulent flow, which ultimately leads to a boundary layer that is thicker and more turbulent. As a direct consequence of this, the increased turbulent activity results in a rise in the skin friction drag, which in turn reduces the overall efficiency of the flow. The added complexity imposed by the three-dimensional structure of the flow causes the impacts of surface roughness to be more obvious in 3D boundary layers. This is due to the fact that the effects of surface roughness are amplified. Because of the surface's imperfections, the spanwise flow patterns are disrupted, which in turn leads to an increase in momentum transfer, improved mixing, and changed pressure distributions. Because of these effects, the skin friction drag contributes to greater levels, and the boundary layer becomes more turbulent. In addition, the existence of three dimensions in 3D boundary layers causes the establishment of discrete flow areas all around the roughness components in the environment. Because of this separation, discrete zones of flow reversal, higher vorticity, and improved turbulence generation are all produced. As a direct result of this, the unfavorable pressure gradients that exist in these geographically distinct areas further exacerbate the skin friction drag. The comparison research also reveals that the roughness effects on 3D boundary layers tend to be more complicated and elaborate than those on 2D boundary layers. This is because 3D boundary layers are often more complex than 2D boundary layers. A very turbulent and energetically demanding boundary layer is produced as a result of the added complexity that arises from spanwise changes and the interplay between the roughness elements and the three-dimensional flow structures. Both two-dimensional and three-dimensional MFD boundary layers are greatly impacted by the existence of surface roughness. The surface's imperfections encourage an early transition to turbulent flow,

which in turn increases the drag caused by skin friction and changes the flow characteristics. Because of the added complexity brought about by the third dimension, the effects are more obvious in the border layers of a three-dimensional object.These results highlight the necessity of addressing surface roughness effects in the analysis and design of fluid flow systems, as they play an essential part in maximizing both efficiency and performance. This is because surface roughness effects have a direct bearing on the flow of fluids across surfaces. To further increase our knowledge and construct reliable prediction models for practical applications, future study should continue to investigate the complexities of surface roughness impacts on boundary layers. This will allow for better practical applications.

REFERENCES

1. Oerlemans, S., Sijtsma, P., and Méndez López, B., "Location and Quantification of Noise Sources on a Wind Turbine," 2007, pp. 869–883.
2. Zhang, X., "Airframe Noise—High Lift Device Noise," Encyclopedia of Aerospace Engineering, edited by R. Blockley, and W. Shyy, John Wiley & Sons, Ltd., 2010.
3. Moreau, S., "Turbomachinery Noise Predictions: Present and Future," 2018, pp. 92–116. https://doi.org/10.3390/acoustics1010008
4. Moreau, S., and Roger, M., "Advanced Noise Modeling for Future Propulsion Systems," International Journal of Aeroacoustics, 2018, pp. 576–599.
5. Amiet, R. K., "Noise Due to Turbulent Flow Past a Trailing Edge," Journal of Sound and Vibration, 1976, pp. 387–393. https://doi.org/10.1016/0022-460X(76)90948-2
6. Brooks, T. F., Pope, D. S., and Marcolini, M. A., "Airfoil Self-Noise and Prediction," NASA Rept. RP-1218, 1989.
7. Blumer, C. B., and Van Driest, E. R., "Boundary Layer TransitionFreestream Turbulence and Pressure Gradient Effects," AIAA Journal, 6, 1963, pp. 1303–1306. https://doi.org/10.2514/3.1784
8. Wells, C. S., Jr., "Effects of Freestream Turbulence on Boundary- Layer Transition," AIAA Journal, 1967, pp. 172–174. https://doi.org/10.2514/3.3931
9. Herr, M., Ewert, R., Rautmann, C., Kamruzzaman, M., Bekiropoulos, D., Arina, R., Iob, A., Batten, P., Chakravarthy, S., and Bertagnolio, F., "Broadband Trailing-Edge Noise Predictions: Overview of BANC-III Results," AIAA Paper 2015-2847, 2015.
10. Herr, M., and Kamruzzaman, M., "Benchmarking of Trailing-Edge Noise Computations—Outcome of the BANC-II Workshop," AIAA Paper 2013-2123, 2013.
11. Choudhari, M. M., Bahr, C., Khorrami, M. R., Lockard, D. P., Lopes, L., Zawodny, N., Herr, M., A BANC Workshops Perspective," Proceedings of the NATO STO-MP-AVT-246 Specialists Meeting on Progress and Challenges in Validation Testing for Computational Fluid Dynamics, Avila, Spain, Sept. 2016.
12. Klebanoff, P. S., and Tidstrom, K. D., "Mechanism by Which a Two– Dimensional Roughness Element Induces Boundary-Layer Transition," 1972, pp. 1173–1188. https://doi.org/10.1063/1.1694065
13. Saric, W. S., Reed, H. L., and Kerschen, E. J., "Boundary-Layer Receptivity to Freestream Disturbances," Annual Review of Fluid Mechanics, 2002, pp. 291–319. https://doi.org/10.1146/annurev.fluid.34.082701.161921
14. Perraud, J., Arnal, D., Seraudie, A., and Tran, D., "Laminar-Turbulent Transition on Aerodynamic Surfaces with Imperfections," RTO-AVT111 Symposium, Prague, Czech Republic, Oct. 2004.
15. Fransson, J. H. M., Brandt, L., Talamelli, A., and Cossu, C., "Experimental and Theoretical Investigation of the Nonmodal Growth of Steady Streaks in a Flat Plate Boundary Layer," Physics of Fluids, 2004, pp. 3627–3638. https://doi.org/10.1063/1.1773493